

Biodegradable Microwave Cavity Resonator

Bathaei, Mohammad Javad; Hashemizadeh, Sina; Arroyo Cardoso, Filipe; Nikolayev, Denys; Boutry, Clementine M.

DOI

[10.1109/LMWT.2025.3588738](https://doi.org/10.1109/LMWT.2025.3588738)

Publication date

2025

Document Version

Final published version

Published in

IEEE Microwave and Wireless Technology Letters

Citation (APA)

Bathaei, M. J., Hashemizadeh, S., Arroyo Cardoso, F., Nikolayev, D., & Boutry, C. M. (2025). Biodegradable Microwave Cavity Resonator. *IEEE Microwave and Wireless Technology Letters*, 35(11), 1736-1739. <https://doi.org/10.1109/LMWT.2025.3588738>

Important note

To cite this publication, please use the final published version (if applicable).
Please check the document version above.

Copyright

Other than for strictly personal use, it is not permitted to download, forward or distribute the text or part of it, without the consent of the author(s) and/or copyright holder(s), unless the work is under an open content license such as Creative Commons.

Takedown policy

Please contact us and provide details if you believe this document breaches copyrights.
We will remove access to the work immediately and investigate your claim.

**Green Open Access added to [TU Delft Institutional Repository](#)
as part of the Taverne amendment.**

More information about this copyright law amendment
can be found at <https://www.openaccess.nl>.

Otherwise as indicated in the copyright section:
the publisher is the copyright holder of this work and the
author uses the Dutch legislation to make this work public.

Biodegradable Microwave Cavity Resonator

Mohammad Javad Bathaei¹, Sina Hashemizadeh², Filipe Arroyo Cardoso, Denys Nikolayev³,
and Clementine M. Boutry

Abstract—This letter presents the first fabrication and characterization of a biodegradable coaxial cavity resonator, focusing on the measurement of complex permittivity of encapsulation as well as $|S_{11}|$ and impedance parameters. The resonator components are 3D-printed from plant-based resin, coated with silver-coated copper flakes, and enclosed by a laser-cut zinc membrane. A monopole coupler antenna, inspired by the “Great Seal Bug,” is co-designed with the cavity to enable near-field coupling and achieve frequency-selective, near-50 Ω impedance-matched wireless sensing. Numerical and experimental analysis of the gap between post and membrane (G-post), and between the coupler antenna and post, resulted in $|S_{11}|$ of -30.3 dB at 1.7 GHz, and a quality factor of 307, outperforming existing flat biodegradable resonators. A 40-MHz resonance shift is observed with a 20 μm variation in G-post, highlighting the resonator’s high sensitivity to membrane position. This system enables battery-free wireless sensing with biodegradable antennas for biodiversity monitoring.

Index Terms—3-D printing, biodegradable materials, cavity resonator, laser cutting.

I. INTRODUCTION

PASSIVE sensing and monitoring through backscattering offer significant advantages, enabling wireless, battery-free operation for complex environments, such as dense vegetation areas, biological tissues, or indoor spaces [1]. By combining high- Q resonators for enhanced sensitivity with well-matched, low-loss antennas for efficient signal retro-transmission, these sensors provide an effective solution for environmental sensing and monitoring [2].

Biodegradable sensors that safely decompose into harmless byproducts offer a sustainable solution to the growing problem of electronic waste (E-waste). Their passive, wireless design allows long-range communication and deployment by aerial robots, overcoming the limitations of human-accessible placement. This innovation enhances scalability, enables fully

Received 13 June 2025; accepted 10 July 2025. Date of publication 14 August 2025; date of current version 7 November 2025. This work was supported in part by the 4TU-Program “Green Sensors” through High Tech for a Sustainable Future (HTSF)—4TU is the federation of the four technical universities in The Netherlands (Delft University of Technology-DUT, Eindhoven University of Technology-TU/e, the University of Twente-UT, and Wageningen University and Research-WUR). (Corresponding author: Clementine M. Boutry.)

Mohammad Javad Bathaei, Filipe Arroyo Cardoso, and Clementine M. Boutry are with the Department of Microelectronics, Delft University of Technology, 2628 Delft, The Netherlands (e-mail: J.Bathaei@tudelft.nl; f.arroyocardoso@tudelft.nl; c.m.f.viellard-boutry@tudelft.nl).

Sina Hashemizadeh is with the Foundation for Research on Information Technologies in Society (IT²S), 8004 Zürich, Switzerland (e-mail: sina@itis.swiss).

Denys Nikolayev is with the Institut d’électronique et des Technologies du numérique (IETR UMR 6164), French National Center for Scientific Research (CNRS)/University of Rennes, 35042 Rennes, France (e-mail: d@deniq.com).

Digital Object Identifier 10.1109/LMWT.2025.3588738

autonomous data collection, and significantly improves spatial resolution in ecological monitoring [3], [4].

Cavity resonators, with their enclosed design, offer high Q -factors and reduced radiation losses, enabling precise, energy-efficient detection that outperforms microstrip [4], split-ring (SR) [5], and dielectric resonator designs [6]. When integrated with antennas, these resonators enable long-range wireless sensing, making them ideal for ecological monitoring applications. However, developing high- Q biodegradable versions is challenging, requiring low-loss biodegradable materials and compatible 3-D fabrication techniques.

A notable historical example is the “Great Seal Bug,” a passive listening device that used a cavity resonator coupled with an antenna to modulate the amplitude of retro-transmitted radio waves via a thin metal membrane, shifting the resonance frequency of the cavity [7], [8]. This concept illustrates how cavity resonators can be leveraged for passive sensing applications requiring high sensitivity and remote operation.

In this letter, we present a biodegradable cavity resonator system fabricated using digital light processing (DLP) 3-D printing. A plant-based ultraviolet (UV)-curable resin serves as the dielectric material to ensure biodegradability. Conductivity is provided by spray-coating with silver-coated copper flakes, while a laser-cut biodegradable zinc membrane is positioned near the post to enable full confinement of the cavity modes. The cavity is characterized by measurements of its complex impedance, demonstrating and its potential for wireless, sustainable microwave sensing.

II. NUMERICAL ANALYSIS

The initial cavity dimensions were replicated from the original “Great Seal Bug” design [9], [10]. However, two key parameters—the gap between the post and membrane (G-post) and between the coupler antenna and post (G-antenna) [Fig. 1(a)]—were not previously defined and analyzed [10]. These were realized as key design variables and analyzed parametrically to evaluate their influence on system impedance and resonance frequency, which were not investigated in the previous analysis of this cavity design [9], [10].

We studied the effect of these gaps on the cavity impedance and its resonance behavior using the frequency domain solver of CST Microwave Studio. As shown in Fig. 1(b), the model was built using the historical device dimensions according to [10], with a coaxial port placed at the end of the coupler antenna.

Initially, the G-antenna was fixed at 1 mm, while the G-post was varied from 0.4 to 1.6 mm. The real part of the impedance exhibited a nonlinear variation, ranging from 0 to 245 Ω

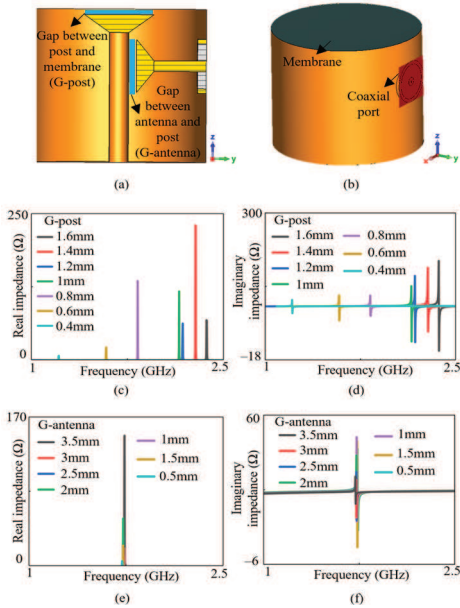


Fig. 1. Numerical modeling of the cavity impedance based on Great Seal Bug dimensions. (a) Cross-sectional view indicating the two critical gaps. (b) Perspective view with a post and a membrane. (c) Real impedance variation for different G-posts. (d) Imaginary impedance variation for a G-posts. (e) Real impedance variation for different G-antennas. (f) Imaginary impedance variation for different G-antennas.

[Fig. 1(c)]. However, the G-post variation significantly affected the resonance frequency, where decreasing the gap from 1.6 to 0.4 mm lowered the resonance frequency from 2.4 to 1.2 GHz [Fig. 1(d)]. This result indicates that even subtle membrane displacements alter the resonance frequency, highlighting its potential as a highly sensitive pressure sensor.

Subsequently, the G-post was set to 0.7 mm, and the G-antenna was varied as shown in Fig. 1(e). Increasing the G-antenna led to a rise in the real part of the impedance, but it did not affect the resonance frequency of the cavity [Fig. 1(f)], indicating its potential for tuning the impedance matching with the antenna.

III. MATERIALS AND FABRICATION PROCESS

The device was fabricated using a soybean oil-based biodegradable resin (Sunlu) for structural components and a silver-coated copper flake aerosol (MG Chemicals) for conductive coating, selected for its low surface resistance ($0.08 \Omega/\text{sq}$ at $50 \mu\text{m}$) and excellent spray compatibility for uniform coverage over complex geometries. A $10\text{-}\mu\text{m}$ -thick biodegradable zinc foil was chosen as the membrane material due to its highest conductivity among biodegradable metals ($1.69 \times 10^7 \text{ S/m}$) and laser processability. The only nonbiodegradable material in the device was the conductive aerosol, which constituted roughly 1% of the total device weight (120 g precoating and approximately 121.2 g postcoating).

The cavity, post, coupler antenna, and fixtures were 3-D printed using a DLP printer (Asiga) with $10\text{-}\mu\text{m}$ resolution [Figs. 2(a) and 3(a)]. Postprinting, parts were UV-cured with $5\text{-J}/\text{cm}^2$ dosage and spray-coated three times (10-s each) with silver-coated copper flakes, followed by oven curing at 65°C for 30 min [Figs. 2(b) and 3(b)]. The zinc foil for cavity

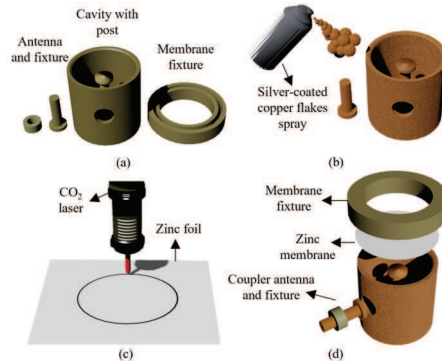


Fig. 2. Step-by-step fabrication of the biodegradable cavity resonator and full device 3-D rendered images. (a) 3-D printing of cavity, post, coupler antenna, and fixtures. (b) Spray coating of silver-coated copper flakes. (c) Laser cutting of zinc foil. (d) Exploded view of all components.

closure was laser-cut (Trotec laser, CO_2 source, 18-W power, 6-mm/s velocity, and single pass) [Fig. 2(c)] and secured using a height-adjustable membrane fixture [$10\text{-}\mu\text{m}$ adjustment, Figs. 2(d) and 3(b)]. This ensured a stable resonance frequency by maintaining a uniform membrane-to-post gap. In addition, the fixture kept the membrane stretched and flat to prevent variations in resonance frequency.

A monopole coupler antenna based on the Seal Bug design [9] was inserted into the cavity for the impedance measurements. Only the section extending into the cavity and terminated with a connector was used to measure cavity impedance. The 3D-printed cavity and post, made from biodegradable resin, are shown in Fig. 3(a) and (b).

The dielectric properties of the 3D-printed samples were characterized using an open-ended coaxial probe technique [11]. As shown in Fig. 3(c), the complex relative permittivity (ϵ_r^*) of the 3D-printed resin at 1.7 GHz is $3.153 - j0.097$, and the loss tangent $\tan(\delta)$ is 0.0309 ± 0.0006 , as shown in Fig. 3(d). The relative permittivity ϵ' is comparable to the polycaprolactone ($\epsilon' \approx 3.3$ and $\tan(\delta) \approx 0.057$), but with lower loss [12], and higher than poly(lactic acid) (PLA) ($\epsilon' \approx 2.9$, $\tan(\delta) \approx 0.01$) [13], and polyhydroxybutyrate (PHB) ($\epsilon' \approx 2.13$) [14].

IV. EXPERIMENTAL CHARACTERIZATION

To determine the resonance frequency of the cavity, a coaxial cable was attached to the antenna coupler using silver paste, connecting its pin to the coupler antenna and grounding it to the cavity outer body [Fig. 4(a)]. The initial cavity, based on original dimensions provided in [9], was not matched to 50Ω . To achieve impedance matching, various coupler antennas, fixtures, and G-antenna configurations were tested.

Since the G-antenna depended on the coupler antenna length, five lengths (1, 1.5, 2, 2.5, and 3 mm) were fabricated. In addition, fixtures with an outer diameter of 5.7 mm and inner diameters of 0.6, 1.1, and 1.6 mm were designed to fit the coupler antenna. Different coupler antenna lengths and diameters were connected to the cavity with a fixed G-post, and the complex impedance was measured.

The optimal configuration for $50\text{-}\Omega$ matching was determined to have a 1-mm antenna diameter, a 5.7-mm fixture outer diameter, a 2-mm G-antenna, and a G-post of 1.5 mm, controlled by the membrane fixture height. As shown in

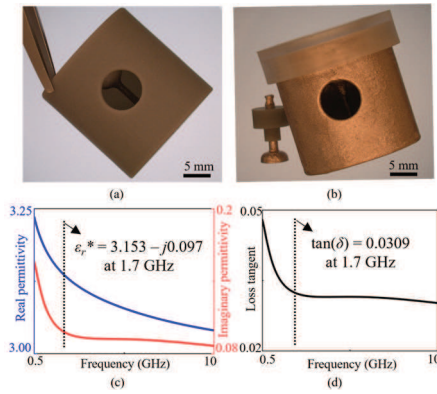


Fig. 3. Photographs and characterization of the device. (a) 3D-printed cavity with post. (b) Silver-coated copper flakes coated the cavity with post, coupler antenna, membrane, and antenna fixtures. (c) Real (ϵ') and imaginary (ϵ'') permittivity of 3D-printed and cured biodegradable resin over frequency. (d) Loss tangent $\tan(\delta)$ of the printed and cured plant-based resin over frequency.

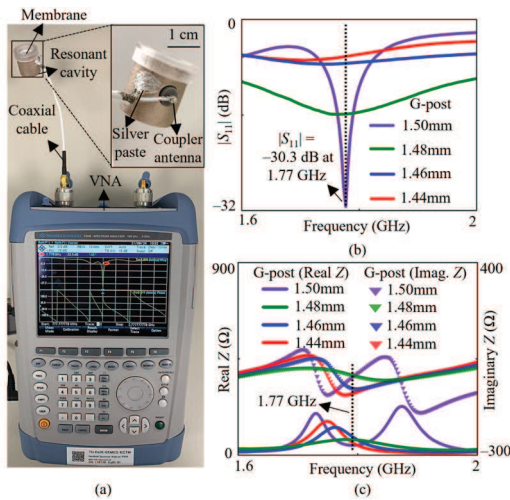


Fig. 4. $|S_{11}|$ and real/imaginary impedance (Z) measurements of the biodegradable cavity resonator. (a) Measurement setup showing the cavity with a topped membrane connected to the VNA. (b) $|S_{11}|$ measured over frequency for different G-posts. (c) Real/imaginary impedance change over frequency for different G-posts.

Fig. 4(b), the measured $|S_{11}|$ exhibits a minimum magnitude of -30.3 dB at a resonance frequency of 1.77 GHz for the G-post of 1.50 mm. A Q -factor of 307, calculated using $Q = f_r/\Delta f$, was achieved through the confined 3-D geometry, a low-loss dielectric, and a tuned membrane gap. This high Q yields a narrowband cavity response, enhancing energy storage and antenna coupling, resulting in a stronger backscatter signal and greater sensitivity to small membrane displacements through distinct shifts in the antenna's reflection response [15], [16].

Subsequently, to investigate the impact of the G-post on impedance, membrane fixtures with $20\text{-}\mu\text{m}$ step increments were 3D-printed, resulting in G-posts of 1.48, 1.46, and 1.44 mm. A $20\text{-}\mu\text{m}$ change in a G-post height resulted in a pronounced variation in $|S_{11}|$ [Fig. 4(b)], with a 40-MHz resonance shift observed between two configurations, featuring a sensitivity of approximately 2 MHz/ μm . This shift was measured using a vector network analyzer (VNA). To highlight this improvement, Table I compares the Q -factor of our resonator

TABLE I
COMPARISON WITH STATE-OF-THE-ART DESIGNS

Resonator Design	Material	Q^1	Geometry-Membrane	Application (Sensor)	Ref.
RLC Tank	PCL ² /Fe ³	~ 100	Planar-NM ⁴	N/A	[17]
	PLA/ Mo ⁵	~ 90	Planar-NM	N/A	[18]
Split-ring	PLA/Ag ⁶	~ 75	Planar-NM	Chemical	[19]
	PLA/Mg ⁷	~ 65	Planar-NM	pH	[5]
Microstrip	Wax/Cu ⁸	~ 50	Planar-NM	RH ⁹	[20]
	PLA/Zn ¹⁰	~ 60	Planar-NM	Moisture	[4]
Dielectric	PLA-PHB	N/A	3D-NM	Temp.	[21]
Proposed Cavity	Resin/Ag-Cu	307	3D-M ¹¹	Pressure (sound)	TW

¹ Q : Quality Factor; ² PCL: Polycaprolactone; ³ Fe: Iron; ⁴ NM: No Membrane; ⁵ Mo: Molybdenum; ⁶ Ag: Silver; ⁷ Mg: Magnesium; ⁸ Cu: Copper; ⁹ RH: Relative Humidity; ¹⁰ Zn: Zinc; ¹¹ M: Membrane-based

with existing biodegradable designs. This is the first 3-D biodegradable resonator incorporating both a membrane and a high quality factor, offering strong potential for applications requiring high sensitivity.

Since the resonators do not necessarily need to be matched to $50\ \Omega$ (but rather to the antenna), the real and imaginary impedance serve as more relevant metrics for device design. The measured impedance is shown in Fig. 4(c). At 1.77 GHz, the resonator with a G-post of 1.50 mm exhibits an impedance of $46.3 - j7.09$, indicating near-optimal matching to $50\ \Omega$, which facilitates measurements with a VNA at this stage. Reducing the G-post shifts the resonance frequency lower, validating the simulation results.

V. CONCLUSION

This letter presents the first biodegradable microwave cavity resonator, fabricated via DLP 3-D printing using plant-based resin, metallic spray coating, and laser cutting a zinc membrane. The device achieved near- $50\ \Omega$ matching at 1.77 GHz with a high Q -factor of 307, outperforming prior biodegradable resonators and demonstrating strong sensitivity to a membrane displacement for precise pressure sensing. However, the current design has limitations, including a nonbiodegradable conductive layer ($\sim 1\%$ of total mass), the need for encapsulation to control degradation, and operation at 1.77 GHz, which lies outside standard ISM bands. Its high- Q cavity enables precise detection of narrow frequency shifts but prevents dynamic tuning across a wide frequency spectrum. Future work will address these through the design and fabrication of fully biodegradable, broadband or tunable antennas, eco-friendly coatings (e.g., zinc or magnesium) [22], and optimization for common bands, such as 434, 868, 915 MHz, and 1.4 GHz [Wireless Medical Telemetry Service (WMTS)]. These advancements will enable a fully passive, battery-free, biodegradable wireless sensing system that uses backscatter communication for biodiversity monitoring through audio sensing. Designed for deployment in natural environments via aerial robots, the system enhances the scalability and autonomy of ecological monitoring while addressing E-waste concerns and broadening the potential of sustainable wireless sensing technologies.

REFERENCES

- [1] Í. V. Soares et al., “Wireless powering for long-lasting deep-body bioelectronic devices: Solutions, limitations, and new technologies [bioelectromagnetics],” *IEEE Antennas Propag. Mag.*, vol. 67, no. 3, pp. 74–86, Jun. 2025, doi: [10.1109/MAP.2024.3482974](https://doi.org/10.1109/MAP.2024.3482974).
- [2] U. S. Toro, K. Wu, and V. C. M. Leung, “Backscatter wireless communications and sensing in green Internet of Things,” *IEEE Trans. Green Commun. Netw.*, vol. 6, no. 1, pp. 37–55, Mar. 2022, doi: [10.1109/TGCN.2021.3095792](https://doi.org/10.1109/TGCN.2021.3095792).
- [3] S. S. Sethi, M. Kovac, F. Wiesemüller, A. Miriyev, and C. M. Boutry, “Biodegradable sensors are ready to transform autonomous ecological monitoring,” *Nature Ecology Evol.*, vol. 6, no. 9, pp. 1245–1247, Jul. 2022, doi: [10.1038/s41559-022-01824-w](https://doi.org/10.1038/s41559-022-01824-w).
- [4] S. Gopalakrishnan et al., “A biodegradable chipless sensor for wireless subsoil health monitoring,” *Sci. Rep.*, vol. 12, no. 1, p. 8011, May 2022, doi: [10.1038/s41598-022-12162-z](https://doi.org/10.1038/s41598-022-12162-z).
- [5] K. Sakabe, T. Kan, and H. Onoe, “Entirely biodegradable wireless pH sensor with split-ring resonators for soil pH monitoring,” *Adv. Mater. Technol.*, vol. 9, no. 13, May 2024, Art. no. 2400038, doi: [10.1002/admt.202400038](https://doi.org/10.1002/admt.202400038).
- [6] P. Sharma, L. Lao, and G. Falcone, “A microwave cavity resonator sensor for water-in-oil measurements,” *Sens. Actuators B, Chem.*, vol. 262, pp. 200–210, Jun. 2018, doi: [10.1016/j.snb.2018.01.211](https://doi.org/10.1016/j.snb.2018.01.211).
- [7] S. Hemour, N. Barbot, F. Collin, J.-L. Lachaud, S. Destor, and J. Tomas, “The great microwave education opportunity of the great seal bug (also known as ‘the thing’),” in *Proc. 54th Eur. Microw. Conf. (EuMC)*, Paris, France, Sep. 2024, pp. 72–75.
- [8] A. Akkoç, “Design and implementation of a microwave cavity resonator for modulated backscattered wave,” M.S. thesis, Dept. Electron Eng., Middle East Tech. Univ., Ankara, Turkey, 2015.
- [9] G. Brooker and J. Gomez, “Lev Termen’s great seal bug analyzed,” *IEEE Aerosp. Electron. Syst. Mag.*, vol. 28, no. 11, pp. 4–11, Nov. 2013, doi: [10.1109/MAES.2013.6678486](https://doi.org/10.1109/MAES.2013.6678486).
- [10] J. W. Ford, “Drawing and photographs of the Russian resonant cavity microphone,” FBI Lab., Washington, DC, USA, Tech. Rep. E. O. 13526, 1952.
- [11] A. Fallahi, S. Hashemizadeh, and N. Kuster, “On the dielectric measurement of thin layers using open-ended coaxial probes,” *IEEE Trans. Instrum. Meas.*, vol. 70, pp. 1–8, 2021, doi: [10.1109/TIM.2021.3123257](https://doi.org/10.1109/TIM.2021.3123257).
- [12] J. Tu, C. Chu, Y. Gao, Z. Wang, P. Xu, and Y. Ding, “Enhanced dielectric and mechanical properties of polylactic acid/polycaprolactone blends by introducing double-layer carbon nanofillers,” *J. Appl. Polym. Sci.*, vol. 141, no. 5, p. 54874, Feb. 2024, doi: [10.1002/app.54874](https://doi.org/10.1002/app.54874).
- [13] P. U. Linge et al., “Evaluation of polylactic acid polymer as a substrate in rectenna for ambient radiofrequency energy harvesting,” *J. Low Power Electron. Appl.*, vol. 13, no. 2, p. 34, May 2023, doi: [10.3390/jlpea13020034](https://doi.org/10.3390/jlpea13020034).
- [14] T. Fahmy, M. T. Ahmed, A. El-Kotp, H. G. Abdelwahed, and M. Y. Alshaer, “Broadband dielectric spectroscopy and electric modulus analysis of poly (3-hydroxybutyrate-Co-3-hydroxyvalerate) and related copolymers films,” *Int. J. Phys. Appl.*, vol. 8, no. 1, pp. 1–14, Dec. 2016, doi: [10.33545/26647575](https://doi.org/10.33545/26647575).
- [15] K. F. Alsirhani, K. A. Abdalmalak, C. S. Lee, A. A. Althwayb, V. G. Posadas, and L. E. G. Muñoz, “Enhancement of gain and bandwidth of cylindrical dielectric resonator antenna excited by cavity-backed slot,” *Alexandria Eng. J.*, vol. 104, pp. 480–489, Oct. 2024, doi: [10.1016/j.aej.2024.07.129](https://doi.org/10.1016/j.aej.2024.07.129).
- [16] S. Su et al., “Slot antenna integrated re-entrant resonator based wireless pressure sensor for high-temperature applications,” *Sensors*, vol. 17, no. 9, p. 1963, Aug. 2017, doi: [10.3390/s17091963](https://doi.org/10.3390/s17091963).
- [17] C. M. Boutry, H. Chandralim, P. Streit, M. Schinhammer, A. C. Hänzi, and C. Hierold, “Characterization of miniaturized RLC resonators made of biodegradable materials for wireless implant applications,” *Sens. Actuators A, Phys.*, vol. 189, pp. 344–355, Jan. 2013, doi: [10.1016/j.sna.2012.08.039](https://doi.org/10.1016/j.sna.2012.08.039).
- [18] M. J. Bathaei et al., “Photolithography-based microfabrication of biodegradable flexible and stretchable sensors,” *Adv. Mater.*, vol. 35, no. 6, pp. 1–13, Feb. 2023, doi: [10.1002/adma.202207081](https://doi.org/10.1002/adma.202207081).
- [19] A. Salim, S. Ghosh, and S. Lim, “Low-cost and lightweight 3D-printed split-ring resonator for chemical sensing applications,” *Sensors*, vol. 18, no. 9, p. 3049, Sep. 2018, doi: [10.3390/s18093049](https://doi.org/10.3390/s18093049).
- [20] J. Bourely, L. De Sousa, N. Fumeaux, O. Vorobyov, C. Beyer, and D. Briand, “Biodegradable materials as sensitive coatings for humidity sensing in S-band microwave frequencies,” *Micro Nano Eng.*, vol. 19, Jun. 2023, Art. no. 100185, doi: [10.1016/j.mne.2023.100185](https://doi.org/10.1016/j.mne.2023.100185).
- [21] D. Vimukthi, E. Jayamani, K. Soon, J. Subramanian, and R. Ravi Sankar, “Analysis of dielectric resonator antenna using natural fiber reinforced polymer composites,” *Mater. Today, Proc.*, vol. 103, pp. 346–351, Sep. 2024, doi: [10.1016/j.matpr.2023.08.363](https://doi.org/10.1016/j.matpr.2023.08.363).
- [22] A. Yue, Y. Cao, Y. Zhang, and S. Zhou, “Study of electroless-deposited Zn on the surface of Mg-Li alloy,” *Materials*, vol. 16, no. 16, p. 5511, Aug. 2023, doi: [10.3390/ma16165511](https://doi.org/10.3390/ma16165511).